Chapter 1

Introduction

In this chapter we introduce the topic to the reader and give the motivation for the work undertaken in the thesis. We provide a literature survey for the background.

1.1 Overview

The advancement in science and technology and better understanding of material behavior have enabled development of materials which apart from displaying usual properties (mechanical, thermal, electrical etc.) also show additional functional capabilities (sensing, actuation, electromagnetic shielding etc.). These are called multifunctional materials. A specialized subgroup of these materials exhibiting sensing and actuation capabilities are known as active materials. They can be used for sensing purpose (e.g. thermal, mechanical, magnetic, optical input →voltage output) or as actuator (e.g. thermal, electrical, magnetic, optical input → mechanical output). Some examples of active materials include piezoelectric and electrostrictives (coupling of mechanical with electric fields), piezomagnetics and magnetostrictives (coupling of mechanical with magnetic fields), and shape memory materials (coupling of thermal with mechanical fields). In these materials the external field directly couples to the actuation like in piezoceramics, piezoelectric polymers, magnetostrictive ceramics, shape memory alloys and magnetic shape memory alloys. Faster response time and enhanced actuation stress are the main advantages of these active materials.

1.2 Shape memory effect

Shape Memory Alloys (SMA) is a class of shape memory materials with the ability to recover their shape reversibly when the temperature is increased. An increase in temperature can result in shape recovery even under high applied loads therefore resulting in high actuation energy densities. SMA's develop the largest strains of the actuator materials available till date and thus these materials have been in the forefront of research ever since their discovery [1]. These materials have been adapted into wide variety of industrial sectors such as aerospace, naval, automotive, biomedical, etc. [2,3]. The irreversible martensitic transformation was first observed back in 1890s by Adolf Martens in Fe-C system. The shape memory effect which occurs as the result of thermally induced reversible transformation of martensite was first observed in 1949 in CuZn and CuAl alloys [2]. A first-order diffusionless structural phase transition from the high temperature austenite phase to the low temperature martensite phase, known as

martensitic transition (MT) which occurs via shear lattice distortion, plays the key role in the shape memory effect.

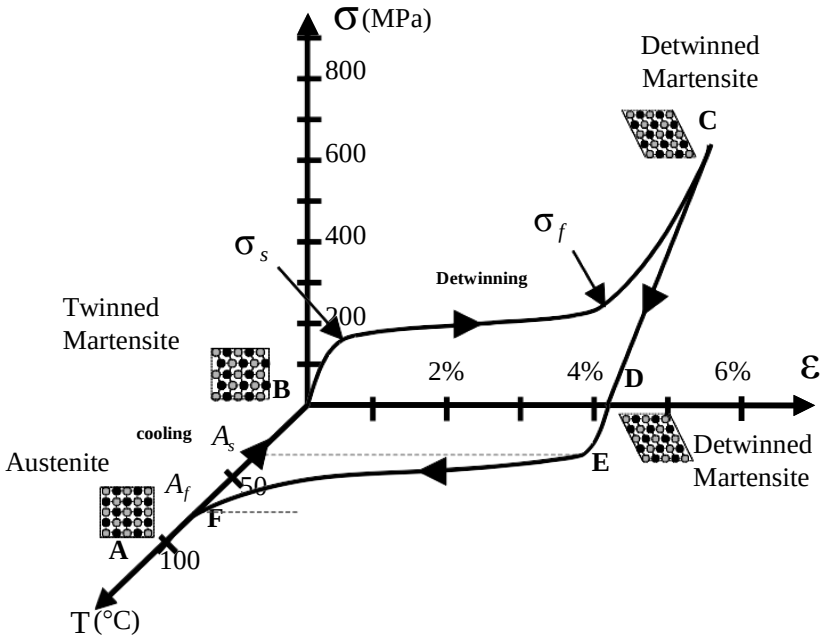

Figure 1.1 Stress-strain-temperature data exhibiting the shape memory effect for a typical NiTi SMA [3].

As the sample is cooled during the forward transformation, austenite or the parent phase with higher symmetry begins to transform to lower symmetric twinned martensite at the martensitic start temperature (M_S) and completes transformation at the martensitic finish temperature (M_F). During heating, the reverse transformation initiates at the austenitic start temperature (A_S) and completed at the austenitic finish temperature (A_F). The crystal in martensitic phase has lower symmetry and is thus degenerate, which results in a certain number of structures which are energetically equivalent but with different crystallographic orientations: these are called variants. These martensitic variants can exist either as a twinned martensite, which is formed by a combination of self-accommodated martensitic variants to minimize the elastic energy, or as a detwinned or reoriented martensite in which a specific variant is dominant. Detwinning can be induced by applying stress; the minimum stress required for detwinning initiation is termed as the detwinning start stress (σ_s) and at sufficiently high stress which results in complete detwinning of martensite is called the detwinning finish stress (σ_f). The detwinning

results in macroscopic shape change. Reheating the material will result in transformation back to parent phase and shape recovery even while the load is still applied. The schematic described above has been shown in the Figure 1.1 (figure has been taken form Ref [3]).

The transformation to martensitic phase can also be induced by applying sufficient external stress at a temperature above A_F. The external stress result in formation of fully detwinned martensite created from austenite and complete shape recovery is observed upon unloading to austenite. This effect is known as superelasticity.

1.3 Ferromagnetic shape memory alloy

The discovery of the magnetic shape memory alloys, often referred to as ferromagnetic shape memory alloys (FSMA), has further increased interest in these class of alloys as their shape memory properties can be controlled by magnetic field apart from the thermal and stress control [4,5]. The shape memory effect occurs due to detwinning of martensitic variants by applied stress, which is controlled thermally thus actuation frequency is limited due to rate of heat transfer. In FSMA actuation is achieved additionally by magnetic field thus working frequency is much higher [6].

There exist strong coupling between mechanical and magnetic properties of FSMA, which makes them important in applications like sensors and actuators. The most widely investigated magnetic shape memory materials have been Ni-Mn-Z (where Z = Al, Ga, In, Sn and Sb). Several other types of FSMA has been studied which include Co-Ni-Al [7], Fe-Pt [8], Co-Ni-Ga [9] and Ni-Fe-Ga [10]. These alloys other than Ni-Mn-Z (except for Z= Al) systems exhibit lower functionality as compared to Ni-Mn-Z system but have higher ductility and mechanical properties. However work presented here is focused on Ni-Mn-Z system. We will discuss various properties of FSMA system based on this system.

1.3.1 Magnetic shape memory effect

In FSMA the twin variants have preferred directions of magnetization below the Curie temperature [4,5]. When a magnetic field is applied and if the magnetic anisotropic energy is less than the energy required to move a twin boundary then magnetization

within each variant changes and no shape change is observed as shown in the Figure 1.2. However if the magnetic anisotropy is high and the energy required to move twin boundaries is low enough, there will be a rotation of the structural domains in such a way that their easy axes get aligned along the externally applied field. In this case, the rotation of martensitic variants is promoted by the difference in the Zeeman energy between the variants, and thus results in a significant macroscopic shape change as shown in the Figure 1.2 and shape can be recovered once the field is removed [11–13].

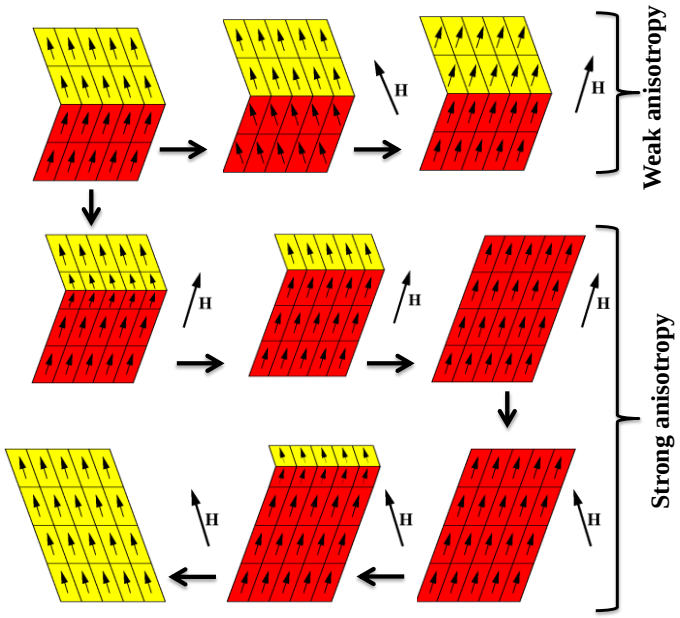

Figure 1.2 Rearrangement of the martensite variants in the magnetic field (H) when magnetocrystalline anisotropy is weak and when it is strong. Favorably oriented variants grow at the expense of unfavorably oriented variants to align the magnetization along applied H [12].

The recovery of shape change upon removal of magnetic field is not complete and it is reversible only for small strain [14,15]. The occurrence of detwinning under applied magnetic field was observed using various experimental techniques [15,16]. The magnetic field induced recoverable strain as high as 10 % has been achieved in FSMA which is two orders of magnitude larger than the magnetic-field-induced strains observed in ordinary magnetostrictive materials, such as Terfenol-D [14]. As actuation in FSMA is driven by the magnetic-field-induced reorientation of martensitic variants, it has much higher operating frequency compared to SMA, but they suffer from low blocking stress level above which magnetic-field-induced strains are completely suppressed [17].

In FSMA a strong coupling exists between the structure and magnetic moments, which modifies the relative stability of austenitic and martensitic phases. The application of field stabilizes phases having higher magnetism. This lead to dependence of MT temperature on the applied field and depending on the whether the martensitic has higher or lower magnetization than the austenitic phase, either the forward or the reverse MT is promoted by application of field. This condition is expressed by Clausius-Clapeyron equation. This leads to magnetic superelasticity in FSMA where large strain is achieved by applying magnetic field that induces MT and on removal of field reverse transition takes place with recovery of strain. Similarly reverse magnetic superelasticity is also observed when field induces austenitic transformation, this is more commonly known as metamagnetic shape memory [18]. The metamagnetic behavior is found in several Ni-Mn-Z alloys, while the Ni-Mn-Ga system shows magnetic superelasticity [19]. The Ni-Mn-In [15] and Ni-Mn-Sn [20] system generally shows metamagnetic shape memory.

1.3.2 Structure of Ni-Mn based alloy

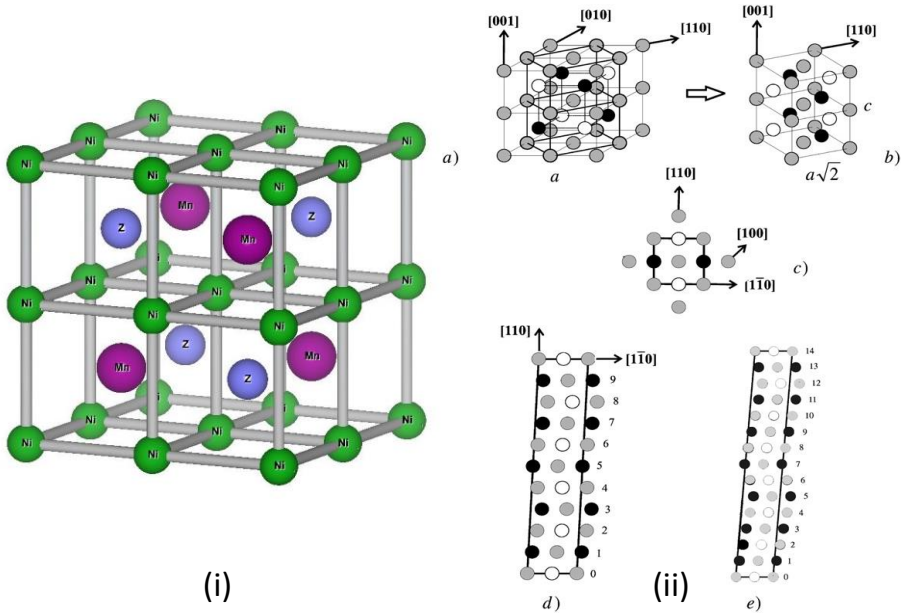

Figure 1.3 (i) The L2 structure for Ni_2MnZ in austenitic phase. (ii) Austenite and martensite structures in case of Ni_2MnGa. Grey: Ni, black: Mn, B white: Z. (a) The $L2_1$ structure showing the relationship with the tetragonal unit cell which is also shown in part (b). (c) The tetragonal unit cell viewed from the top and (d) the 5M (or 10M) and (e) 7M (or 14M) modulated structures obtained by shearing the tetragonal cell [15].

The alloy system we investigated belongs to family of full Heusler alloy. We will refer to

it as Heusler alloy further on. Thus we have given a brief overview of crystal structure of the Heusler alloy. In stoichiometric composition Heusler alloys have the general formula X_2YZ, here X (Ni) and Y (Mn) are transition metal elements and Z (Al, Ga, In, Sn and Sb) is an s-p group element. The austenitic phase is in general higher symmetric phase with $L2_1$ structure having space group *Fm-3m*. This structure has four interpenetrating face centered cubic (fcc) sub-lattices. The sub-lattices with Wyckoff coordinates (0, 0, 0) and (1/2, 1/2, 1/2) are occupied by X atoms, while the sub-lattices with coordinates (1/4, 1/4, 1/4) and (3/4, 3/4, 3/4) are occupied by the Y and Z atoms, respectively. The $L2_1$ cell for Ni_2MnZ is shown in Figure 1.3 (i). When the positions (1/4, 1/4, 1/4) and (3/4, 3/4, 3/4) are randomly occupied by Y and Z the system reduces to B2 type structure and when X, Y and Z atoms occupy all the coordinates randomly then the system is reduced to A2 type.

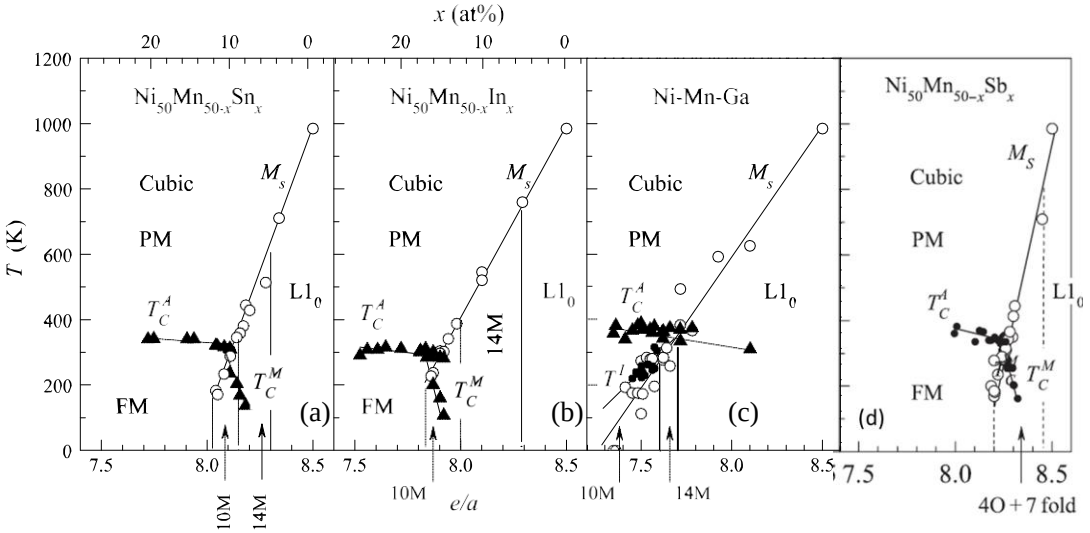

Figure 1.4 The magnetostructural phase diagram of Ni–Mn–Z Heusler alloys with Z as (a) Sn, (b) In, (c) Ga and (d) as Sb. The triangles and the circles correspond to the magnetic and martensitic transformation temperatures respectively. The regions corresponding to the different structures are separated by discontinuous lines. Small solid circles in (c) correspond to the premartensitic transition temperature [15,24].

When temperature is reduced the system undergoes MT to lower symmetric martensitic phase and acquires a number of structures. In general the Ni-Mn-Z system crystallizes in martensitic phase into tetragonal, orthorhombic and monoclinic or into their modulated phases like modulated tetragonal etc. [21–23]. For lower concentration of Z it transforms to the $L1_0$ tetragonal structure, which also happens to be its ground state structure for its

parent compound Ni_2Mn_2. Modulated structures are found at higher concentration of Z and are commonly in 5M or 7M modulations. Martensitic structure in general is formed by the diffusionless tetragonal distortion of initial cubic lattice as shown in the Figure 1.3 (ii a) and the tetragonal structure is shown separately in Figure 1.3 (ii b) (part of Figure 1.3 was taken from [15]). From the X-ray it was further confirmed that the martensitic has monoclinic unit cell constructed of several layers of atomic planes along a particular direction. M refers to the modulation and the number refers to the periodicity of shuffling. Examples of 5M (or 10 M) and 7 M (or 14 M) are shown in the Figure 1.3 (ii d) and (ii e), unit cell is viewed form the top.

While the Ni-Mn-Ga system undergoes MT in stoichiometric composition, the systems with Z = Al, In, Sn, and Sb undergo MT at off-stoichiometric compositions depending on the Z atom. In the Figure 1.4 (extracted from Refs. [15,24]) we see the evolution of various martensitic structures and there dependence on the concentration and valence electron concentration per atom e/a. The data for Z as Sn, Sb and In are for $Ni_{50}Mn_{50-x}Z_x$ whereas in Ga system it was taken for all possible compositions. We see that in all the samples at low e/a, system is in 10 M structure and transforms to 14 M to $L1_0$ at higher concentrations for Z = Ga, In and Sn. For Ni-Mn-Sb system we observe that structure changes to mixture of 4O (four fold orthorhombic) and 7 fold orthorhombic at lower e/a and becomes $L1_0$ at higher e/a. 10M modulated phase has also been observed in certain compositions of Sb based alloys instead of 4O [25]. It is also seen that presence of various Z elements affects the width of the various modulated structure. Thus e/a ratio and Z element both play important roles in determining the structure of Ni-Mn-based alloys.

1.3.3 Magnetism in Ni-Mn based alloys

The magnetism in the Ni-Mn-Z system and coupling of it to the martensitic transformation play a key role in properties of these alloys. In austenitic phase the system is predominantly in the ferromagnetic (FM) state. The magnetism in the system is believed to come from the Mn atoms as in case of most of Mn based system [26]. The moment of Mn is close to $4\mu_B$ here and is localized. As seen in the section 1.3.2 the Mn

atoms are not in direct contact, the interaction is indirect among the Mn moments and is sensitive to both distance and percentage of X (Mn) and Z elements. The initial analysis of the inelastic neutron scattering by Noda and Ishikawa and Tahuna *et al*. on the Ni_2MnSn, Pd_2MnSn and Cu_2MnAl showed that interaction was long ranged and oscillatory in nature [27,28]. The ferromagnetism arises due to the Ruderman-Kittel-Kasuya-Yoshida (RKKY) exchange interaction, while the origin of antiferromagnetic (AFM) interactions in Heusler alloys with excess Mn is still elusive [29–31]. The study with Monte Carlo simulation shows that the antiferromagnetism is outcome of RKKY interactions between Mn atoms [30]. Alternatively some first principles study propose superexchange interactions arising due to hybridization between Ni 3d and Mn 3d bands as the origin of antiferromagnetic interactions [26,32].

In austenitic phase the interaction among the Mn-Mn in regular Mn site is ferromagnetic and the interaction is weakly antiferromagnetic between the Mn-Mn atoms in Mn site and Mn in the Z site. The antiferromagnetic interaction is sensitive to distance and it is enhanced at shorter distance [33,34]. The structural transformation to martensitic phase shortens the lattice parameter in one dimension so that the Mn-Mn distance becomes less, ($c_{mar} = c_{aus}/\sqrt{2}$) thus the AFM interaction among Mn-Mn atom in Mn site and Mn in the Z site is enhanced. However, in another dimension the Mn-Mn distance is increased ($a_{mar} = \sqrt{2}a_{aus}$), thus preserving the ferromagnetic character. The resulting magnetic state of the martensitic phase has competing FM-AFM interaction leading to observation of properties like spin glass and exchange bias effect [24,35–38].

The magnetic states of the austenitic and martensitic phase are shown as the function of e/a in Figure 1.4, where T_C^A and T_C^M are the Curie temperatures of austenitic and martensitic phase. The T_C (will mean T_C^A unless otherwise mentioned) for each Z shows little variation, though it falls with increasing e/a. The fall occurs because of increase in probability of Mn occupying the Z site, where the Mn interacts antiferromagnetically. Also with increase in e/a the Mn-Mn distance decreases which strengthens the AFM interaction [15]. One also observes that T_C increases as the Z changes form In to Sn to Sb, showing that FM is enhanced. The T_C of martensitic phase falls much more rapidly with

increasing e/a (except of Z = Ga), which shows that AFM strengthens as sample composition moves closer to Ni_2Mn_2 which is AFM with Neel temperature of 1200 K.

These systems show a variety of features in thermomagnetization curve depending on measurement protocol. The temperature dependent magnetization measurement M (T) carried out for $Ni_2Mn_{1.36}Sn_{0.32}Al_{0.32}$ sample is shown in Figure 1.5. All Ni-Mn-Z samples show almost similar behavior except for the Ni-Mn-Ga system. The magnetization falls suddenly when sample undergoes MT around 240 K. This sudden change in magnetization gives rise to many interesting properties in the sample like large magnetocaloric effect (MCE) and giant magnetoresistance (MR) at MT.

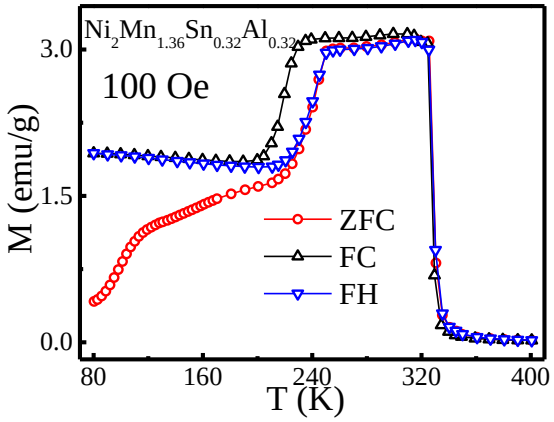

Figure 1.5 Shows thermomagnetization curves measured in zero field cooled (ZFC), field cooled (FC) and field cooled heating (FH) protocols in the dc magnetic field of 100 Oe.

1.3.4 Role of magnetism and ordering on martensitic transformation

The Ni-Mn-Z FSMA alloys in the austenitic phase exist in the $L2_1$ structure. At high temperature the structure has B2 structure which upon cooling transforms to $L2_1$ structure. The transformation to $L2_1$ phase from B2 phase is first order transformation. The B2-$L2_1$ transition takes place at different temperatures for different Z atoms [39–43]. Upon quenching form high temperature (above the B2-$L2_1$ transition temperature), the B2 phase may coexist with $L2_1$ phase as the cooling does not take place at equilibrium. The B2 phase as discussed earlier is disordered phase of $L2_1$ structure where the Mn and Z sites are randomly occupied. Thus more of Mn atoms occupy the Z sites which results in more AFM interaction. The presence of B2 phase thus reduces the overall magnetism of the austenitic phase. The Ni-Mn-Al system has lowest B2-$L2_1$ transition temperature

thus leading to formation of B2 predominantly, thus resulting in austenitic phase with higher AFM interaction. V. Sánchez-Alarcos et al. performed systematic aging on Ni-Mn-In and Ni-Mn-Ga samples starting from temperature below B2-$L2_1$ transition temperature of system till high temperature [44,45]. They showed that the MT temperature and T_C are influenced by aging. While the MT temperature changed only for the system in which one of the phases was ferromagnetic, the system which transformed from a paramagnetic phase to another paramagnetic phase did not display such a shift.

The neutron diffraction study showed that with increasing aging temperature the $L2_1$ fraction in the sample increases. As samples become more ordered higher percentage of Mn atom occupies the Mn site, which in turn results in the enhancement of ferromagnetism of the sample. The change in magnetism of the sample influences the Gibbs free energy of the system. Depending on which phase has higher saturation magnetization the transformation temperature shows negative or positive shift. Overall the structure with higher magnetization gets stabilized with increase in ordering.

1.3.5 Influence of various substitution

FSMA displays a wide variety of properties most of which occur in the vicinity of MT. The transformation is very sensitive to change in e/a, which can be as high as 270 K per 0.1 e/a for Sb system (0.1 e/a corresponds to 2 at. % of Sb) [15] and is also sensitive to the composition. Apart from these the magnetizations of both austenitic and martensitic phases are sensitive to both e/a and composition. Thus an alloy with better functional capabilities may have an operating temperature either too low or too high than room temperature at which most of the devices work.

The transformation temperature can be changed by changing composition which leads to change in e/a ratio of the sample resulting in above effect. Usually with increase in e/a ratio the transformation temperature also reduces [15]. Also the substitution of different elements can bring about the change in the lattice parameters of the system which effects the magnetism thus effecting the stability of phases [44,45]. The substitution can also create chemical hydrostatic pressure which can also bring change in the transformation temperature [35]. Various substitutions have been tried with the aim of both enhancing

the functional capabilities and to bring the transformation temperature close to room temperature. These substitutions also help in understanding the origin of magnetism and MT in these samples.

In the Ni-Mn-Z system (where Z = Al, Ga, In, Sn and Sb) the Z element has been replaced with element like Ge, B, Si and partially with other Z elements [46–51]. In general the substitution of Z with element having small radii results in increase in transformation temperature even if e/a ratio of the system fall, because in most of cases the chemical pressure effect dominates. Boron was introduced in Ni-Mn-Sn system which occupied interstitial site and led to increase in MT, though it also introduced a foreign Mn_2B phase in the system at higher concentration thus reducing magnetocaloric effect [46].

There are also studies where Ni and Mn have been replaced by ferromagnetic elements like Co and Fe and with elements like Cr and Cu. The addition of strong ferromagnetic (Co and Fe) element in the Ni-Mn-Z system breaks the crystallographic symmetry in these systems thereby acting as the "ferromagnetic activator" which turned the antiferromagnetically exchange coupled Mn moments between the Mn in regular site and in Z site into the ferromagnetically exchange coupled ones [52]. The addition of Co doped samples show large change in magnetization at the MT even at room temperature [18,53]. These samples also shows nearly perfect magnetic field induced shape memory effect and the work output stress in these systems is at least one order of magnitude higher than the conventional Ni-Mn-Ga [18,53–55]. The addition of Co results in the metamagnetic shape memory effect in Ni-Mn-Co-Z (where Z is Al, Ga, In, Sn, and Sb) system [52,55–58]. The replacement of the Cr with Mn in Ni-Mn-Sb resulted in enhancement of the FM interaction and suppression AFM interaction though the replacement also leads to drop in values of MR [59].

1.4 Motivation of the work

The Ni-Mn-Z (where Z = Sn, Sb and In) system of alloys though shows a lot of interesting properties as discussed earlier, its main draw backward is brittleness. The

system with Al was proposed as an alternative as the system is more effective for mechanical devices. But Al based system has short coming of its own [60].

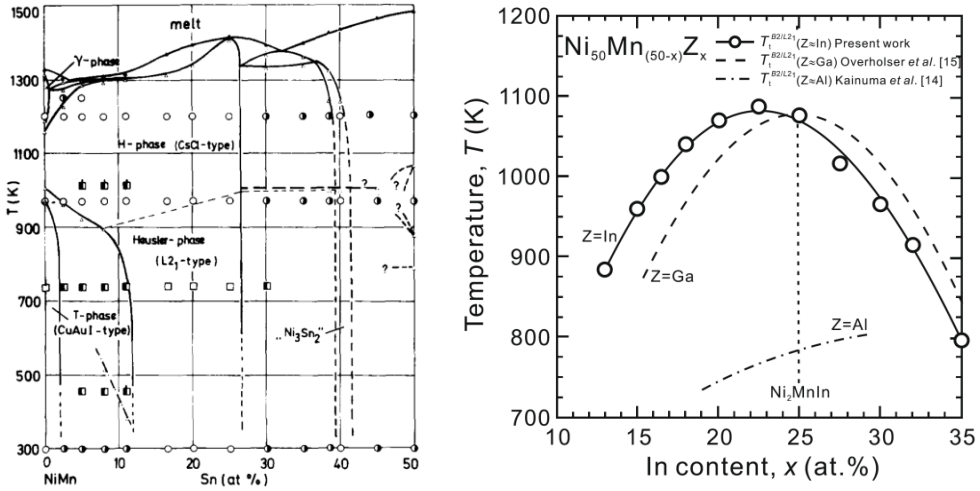

Figure 1.6 (Left) The phase diagram for Ni_2MnSn system showing the B2-$L2_1$ transition temperature (here H-phase is the B2 phase) [39]. (Right) The B2-$L2_1$ transformation determined by the DSC measurements for the Ni_2Mn-In alloys compared with those for the Ni_2Mn-Al and Ni_2Mn-Ga alloys [40].

The Ni-Mn-Al system has a B2 to $L2_1$ ordering temperature in the range of 600 K to 800 K [61]. Thus when Ni_2MnAl system is quenched form high temperature they tend to remain in B2 phase. As said, the main problem with the presence of B2 phase is that it brings more of AFM in the system thus upon structural transformation the change in magnetism is not much. Large values of properties like magnetocaloric effect, magneto-resistance, magnetic field induced stain are usually obtained in the vicinity of structural transformation temperature, where they are driven by large difference in the Zeeman energy of austenitic and martensitic phase [62]. As the change in magnetism is not large the values of these functional properties are much smaller in Ni-Mn-Al system compared to other Ni-Mn-Z (where Z = Sn, Sb and In) [63,64]. It was argued that if more of ordered $L2_1$ phase could be stabilized in the Ni-Mn-Al system then there functional capabilities could be enhanced [64]. Careful and long heat treatments are required at lower (than B2 to $L2_1$ ordering temperature) temperature to stabilize larger fraction of $L2_1$ phase as kinetic of system is very low [64,65].

The presence of Z elements increase the B2-$L2_1$ transition temperature and the system with Z as Sn, In and Ga display much higher B2-$L2_1$ transition temperatures compared to Ni-

Mn-Al system [40,61,66] as shown in the Figure 1.6 (figures were taken from Ref. [39] and [40]). We see from Figure 1.6 that replacement of element like Sn and In with Al can possibly keep the B2-$L2_1$ transition temperature of the system high. Thus obtaining the $L2_1$ phase will become easier even at higher Al content which in turn may lead to better functional capabilities.

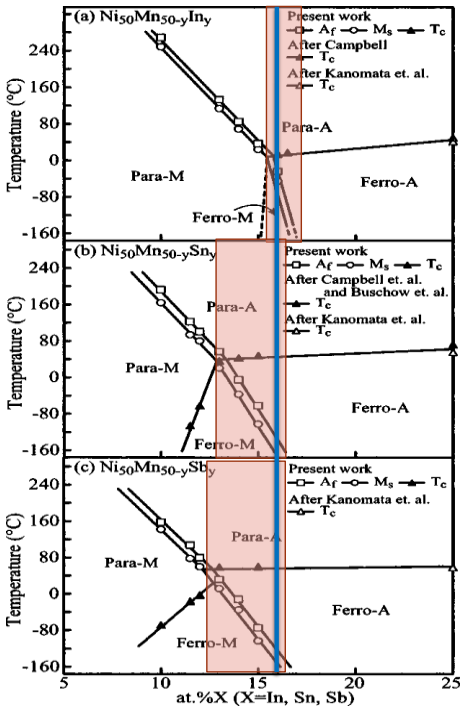

Figure 1.7 Martensitic and magnetic transition temperatures of the (a) $Ni_{50}Mn_{50-y}In_y$, (b) $Ni_{50}Mn_{50-y}Sn_y$ and (c) $Ni_{50}Mn_{50-y}Sb_y$ alloys, where the Para and Ferro mean paramagnetic and ferromagnetic, respectively, and A and M indicate the austenite and martensite phases [67]. The shaded region in red shows the composition for which sample undergoes transition to a magnetic phase and the blue line corresponds to the composition of $Ni_{50}Mn_{34}X_{16}$ ($Ni_2Mn_{1.34}Z_{0.64}$ in our notation).

The Ni-Mn-Z (for Z as Sn, Sb and In) system shows martensitic transformation in the narrow range of composition, in which at least one of the phases has a long range interaction present. The Figure 1.7 which is modification of figure taken form the Ref. [67] shows the shaded region of composition in which at least one phase has long range magnetic interaction. We see that Sn and Sb systems display lowest change in martensitic transformation temperature with change in Z concentration and the region in which sample underwent martensitic transformation to magnetic austenitic or martensitic phase is much broader compared to the Ni_2MnIn system. Based on Figure 1.7 we selected the composition of $Ni_2Mn_{1.34}Z_{0.64}$ (Z is Sn, Sb and In) for the substitution with Al in place of Z as shown

with bold line. As mentioned earlier the substitution of element with having smaller radii increases the transformation temperature even when the e/a ratio decreases. With the replacement of Al in the Z position we expect that the transformation will move to higher temperature and thus we selected the system with Z = 0.64 as it has lowest martensitic transformation temperature with both austenitic and martensitic phase being magnetic.

We have prepared three different series of alloys where we substituted Al in the Z position in $Ni_2Mn_{1.34-x}Z_{x,}$ where Z being Sn, Sb and In and x was varied from 0.24 to 0.40 in the step of 0.04. The samples were characterized using the experimental techniques discussed in the Chapter 2. Their detailed characterization and magnetic properties are discussed in details in the Chapter 3. The functional properties of system like magnetocaloric effect and the exchange bias effect were discussed in details in the Chapter 4. The presence of mixed FM/AFM interaction in the martensitic phase of these systems leads to frustration and freezing at low temperature. We have studied the dynamics of these frozen states using ac and dc magnetic measurement techniques and the effect various substitution has on the dynamics of the system was studied in the Chapter 5. The Ni-Mn-Al system showed better functional capabilities when low temperature heat treatment was performed to enhance the $L2_1$ fraction in the sample. As our systems had large percentage of Al we have performed similar heat treatment study on the selected systems at both low and high temperatures. The effect of heat treatment on the magnetism of the system, magnetocaloric effect and freezing at low temperature was studied and are reported in the Chapter 6. Finally we have compared two of the selected system with the composition $Ni_2Mn_{1.36}Sn_{0.40}Al_{0.24}$ and $Ni_2Mn_{1.36}Sb_{0.40}Al_{0.24}$ as they had identical lattice parameters and concentrations of magnetic Mn atoms, and thus tried to look into the origin of magnetism in these systems in Chapter 7.